Synthesis of Carbon Nanotubes and Nanobelts through a Medial-Reduction Method

Jianwei Liu, Mingwang Shao, Qun Tang, Shuyuan Zhang, and Yitai Qian*

The Structure Research Laboratory, Department of Chemistry, University of Science and Technology of China, Hefei, Anhui 230026, P.R. China

Received: April 4, 2003; In Final Form: May 5, 2003

The method of medial-reduction has been developed for the synthesis of carbon nanotubes and nanobelts. In this process, Mg was used as reductant, and Na_2CO_3 and CCl_4 were used as carbon sources, respectively. X-ray power diffraction (XRD) patterns were used to identify the designed reaction process and carbon structure. Scanning electron microscopy studies showed that as-synthesized products were composed of a large number of carbon nanotubes with diameters of 60−200 nm. Transmission electron microscopy investigations indicated that both types of carbon nanotubes could be observed. Furthermore, carbon nanobelts were found to be coexistent in the as-prepared products. High-resolution transmission electron micrography images showed that as-synthesized carbon materials consisted of graphite layers, whose interlayer spacing was about 0.34 nm. The experimental results indicated that the spiral growth mechanism might be operative during the formation of carbon nanotubes.

Introduction

Carbon nanotubes have recently attracted much attention due to their unique properties and potential applications in numerous areas such as electrochemical devices,[1] hydrogen storage,[2] field emission devices,[3] and nanotweezers.[4] Considerable efforts have been made to study the preparation and growth mechanism of carbon nanotubes.[5−8] For example, carbon nanotubes are usually made by metal catalyzed chemical vapor deposition (CVD),[9] arc evaporation,[10] or laser ablation of carbon.[11] Recent reports indicated that carbon nanotubes could be synthesized from hydrothermal processing[12] or by solid-state metathesis reaction.[13] To explore other alternatives, a solvothermal route has been developed to prepare carbon nanotubes, in which the alkali metals such as K were used as reductants.[14,15] On account of their violently active property, it is inconvenient to employ the alkali metals as initial reagent. Therefore, it is a challenge to utilize mild alkaline-earth metals as reductants to synthesize carbon nanotubes.

Here, we demonstrate that two types of carbon nanotubes have been prepared by using metallic Mg powder as the reductant in the reaction system. In addition, we have found that some carbon nanobelts coexist with carbon nanotubes. Due to the mild property of metallic Mg powder, the reaction can be controlled easily. In the experiment, metallic Mg powder reacts with Na_2CO_3 to produce carbon and sodium. The medial reductant Na may reduce CCl_4 to produce hexagonal carbon clusters. The reaction process can be represented as the following:

$$6Mg + 2Na_2CO_3 + CCl_4 \xrightarrow{500\ ^\circ C} 4NaCl + 6MgO + 3C \quad (1)$$

On the basis of the experimental results, we propose possible mechanisms to illustrate their formation.

Experimental Section

Synthesis of Carbon Material. In a typical experiment, 8 mL of CCl_4 was placed into in a stainless steel autoclave of 12 mL capacity, and 0.30 g of Mg powder and 0.28 g of Na_2CO_3 were added, respectively. The autoclave was sealed and maintained at 500 °C for 10 h and then allowed to cool to room temperature naturally. The dark precipitate was collected and washed with distilled water, dilute HCl aqueous solution, distilled water, and absolute ethanol, respectively. After that, the obtained sample was dried in a vacuum at 65 °C for 5 h. The yield of carbon nanotubes is, estimated through SEM observations, about 35%.

Characterization Techniques. The purity and phase structure of the products were obtained by X-ray powder diffraction (XRD) analysis, which was performed with a Philips X' Pert PRO SUPER diffractmeter using monochrochromatic high-intenstity Cu Kα radiation ($\lambda = 0.154\ 187\ 4$ nm). The morphologies of the samples were observed through scanning electron microscopy (SEM) and transmission electron microscopy (TEM) measurements, which were made on a JEOL JSM-6700F field emission microscope and a Hitachi Model H-800 transmission electron microscope using an accelerating voltage of 200 kV with a tungsten filament, respectively.

The microstructure of carbon nanotubes and nanobelts was analyzed by high-resolution transmission electron microscopy (HRTEM) observation, which was performed with JEOL-2010 transmission electron microscope using an accelerating voltage of 200 kV. Samples for the electron microscope were prepared by ultrasonic dispersion for 1 h of 0.1 g of the as-prepared power with 10 mL of ethanol in a 30 mL conical flask. Then, the suspension was dropped on a carbon-coated copper microgrid and dried in air before performance of the observations.

Information about the vibrational properties of the carbon material was obtained by Raman spectroscopy. The Raman spectrum was recorded at ambient temperature on a Spex 1403 Raman spectrometer with an argon ion laser at an excitation wavelength of 514.5 nm.

Results and Discussion

The X-ray diffraction powder patterns were performed to identify the reaction process (eq 1) mentioned in the Introduction

* To whom correspondence should be addressed. Telephone: +86-551-3601589. Fax: +86-551-3607402. E-mail: ljw@mail.ustc.edu.cn.

10.1021/jp034881i CCC: $25.00
Published on Web 06/07/2003

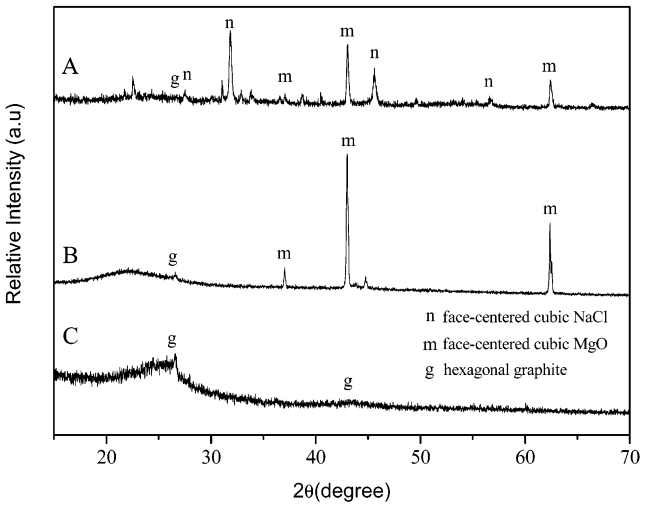

Figure 1. XRD patterns of the products with various treatments: (A) not washed; (B) washed only with distilled water; (C) after HCl treatment.

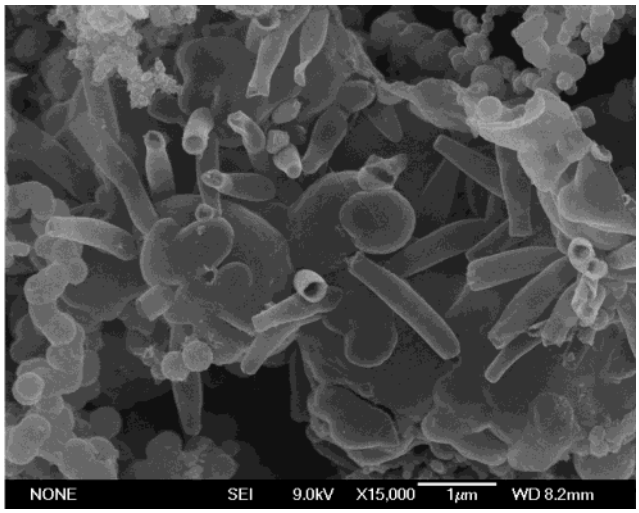

Figure 2. SEM micrographs of as-prepared products.

and the carbon structure. Figure 1A shows the XRD pattern of the products that were not washed. Reflections in the figure can be indexed to face-centered-cubic NaCl (JCPDS Card Files, No. 78-0751), face-centered-cubic MgO (JCPDS Card Files, No. 77-2364), and hexagonal graphite, respectively. The XRD pattern (Figure 1B) from the products washed only with distilled water corresponds to face-centered-cubic MgO and hexagonal graphite. The above results confirm the reaction (eq 1), which occurs according to our design. Figure 1C is a typical XRD pattern of as-prepared products after HCl treatment. The marked peak can be indexed as the (002) and (100) reflections of the hexagonal graphite structure. Compared to the case of ordinary graphite (JCPDS Card Files, No. 41-1487), the XRD intensities of the sample are generally weak and broad, which indicates that nanometer-sized crystallites are formed. At the same time, we also observe that the position of the (002) peak shifts to relatively low 2θ angle, which corresponds to an increase in the spacing between the sp^2-carbon layers.[16] These investigations imply the degree of long-range order of these nanostructures is lower than that of graphite.

Scanning electron microscopy (SEM) images for the as-prepared products are shown in Figure 2. The SEM investigations indicate that a large quantity of carbon nanotubes with diameters of 60−200 nm is formed and some nanotubes have

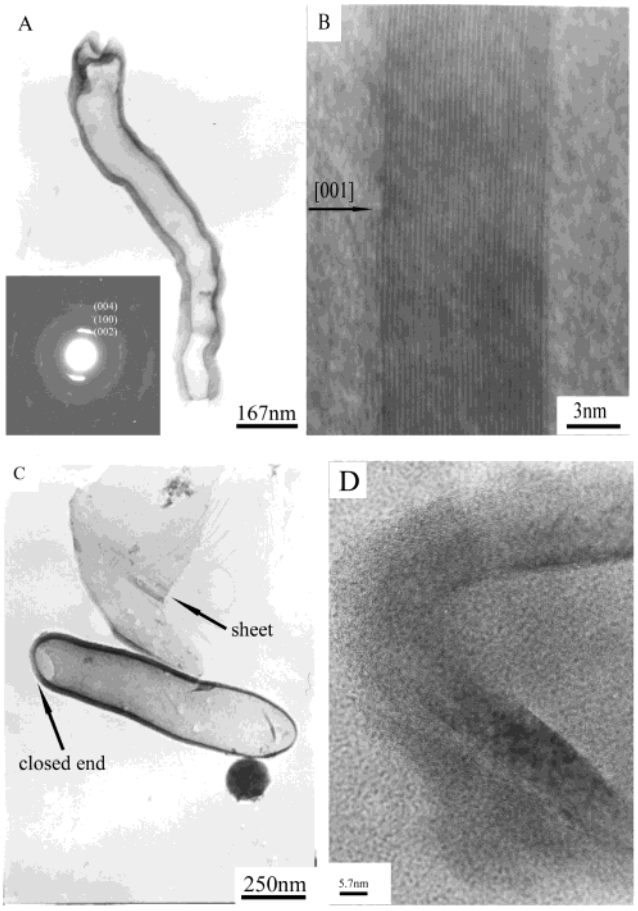

Figure 3. TEM and HRTEM images of carbon nanotubes: (A) a typical nanotube with two open ends (SAED for the nanotube in the inset); (B) HRTEM image of the wall of the nanotube; (C) a carbon nanotube with two closed ends; (D) HRTEM image of a closed end of the carbon nanotube.

open ends. In addition, some particles and sheets can be observed in Figure 2.

A more detailed investigation of as-prepared products by TEM reveals that there are both kinds of carbon nanotubes, a kind of nanotubes with open ends and another with closed ends. The micrographs of the nanotubes are shown in TEM images (Figure 3). From Figure 3A, we can observe that the nanotube has two open ends with a length of 1200 nm. The inner diameter of the nanotubes is 65 nm, and the outer diameter is 80 nm on average. The SAED pattern (inset in Figure 3A) is characteristic of a carbon nanotube with a hexagonal graphite crystalline (JCPDS 41-1487) structure. The rings in the pattern correspond to (002), (100), and (004) planes. This electron diffraction pattern indicates that [001] is the radial direction.

A further analysis by high-resolution transmission electron microscopy (HRTEM) (Figure 3B) reveals that the interlayer spacing of the carbon nanotube is about 0.34 nm, consistent with the (002) plane lattice parameter of graphited carbon.

Figure 3C shows that a carbon nanotube with a length of 1000 nm has two closed ends, as indicated by the arrow. HRTEM observation (Figure 3D) shows that a closed end of a carbon nanotube consists of ∼40 graphite layers with a spacing of about 0.34 nm.

In the processing of TEM and HRTEM examinations of as-prepared products, some carbon nanobelts were detected. Figure 4 shows the TEM and HRTEM images of nanobelts. A typical nanobelt with a thickness of 2 nm, a width of 20 nm, and a length of 500 nm is shown in Figure 4A. High-resolution

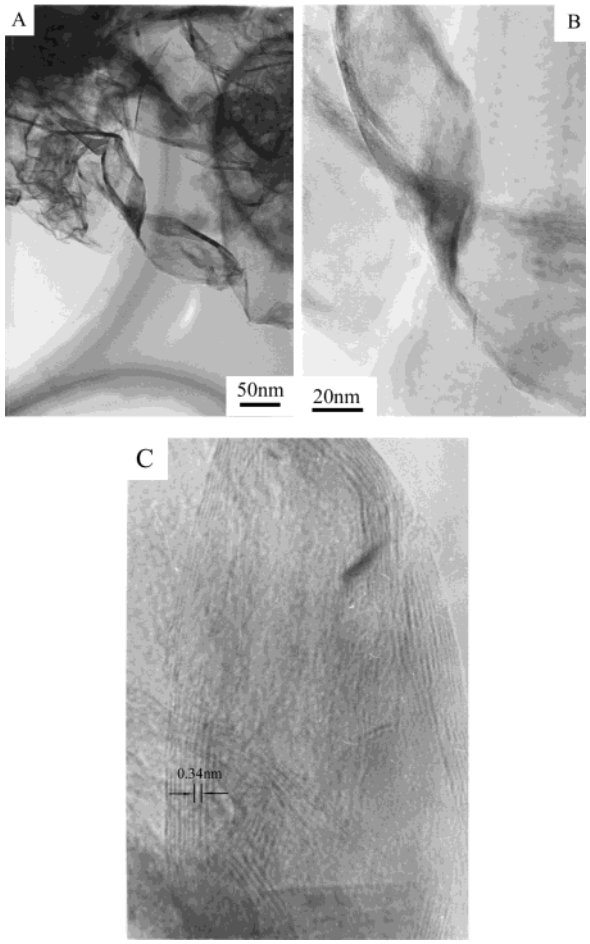

Figure 4. TEM and HRTEM images of carbon nanobelts: (A) a representative nanobelt; (B) enlarged region of the nanobelt; (C) HRTEM image of the nanobelt.

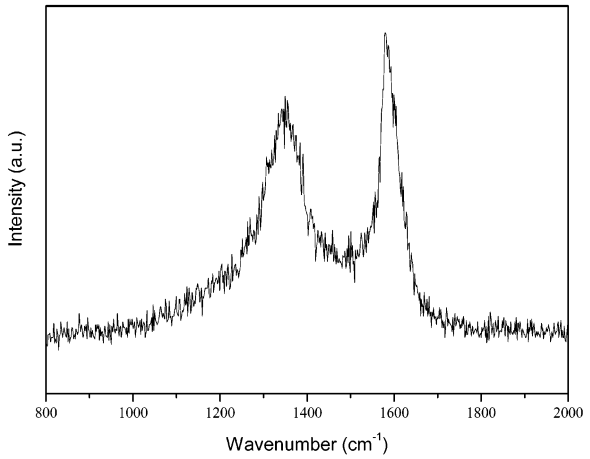

Figure 5. Raman spectrum of as-prepared sample at room temperature (an excitation wavelength of 514.5 nm).

transmission electron microscopy (HRTEM) images (Figure 4C) indicate that the nanobelt is composed of graphite layers with a spacing of up to 0.34 nm.

Raman spectroscopy has been used to investigate the vibrational properties of the as-prepared carbon structure, which also allows us to draw further conclusion about the crystallography or morphology.[17] The typical Raman spectrum (Figure 5) shows that there are two strong peaks at 1350 and 1580 cm^{-1}. The peak at 1580 cm^{-1} (G-band) corresponding to the Raman allowed optical mode E_{2g} of 2-dimensional graphite is closely related to the vibration in all sp^2 bonded carbon atoms in a 2-dimensional hexagonal lattice, such as in a graphite layer. The peak at 1350 cm^{-1} could be assigned to the vibrations of carbon atoms with dangling bonds in plane terminations of disordered graphite. [18] Compared to the early reports,[19] the peak at 1350 cm^{-1} was stronger, suggesting that the products have a lower degree of long-range order.

To investigate the effect of reaction conditions on the formation of carbon nanotubes, a series of relevant experiments were carried out through similar processes. It is obvious that the reaction temperature played a critical role in the formation of carbon nanotubes. Lower temperatures than 300 °C could not initiate the reactions. When the reaction temperature was at 400 °C, the carbon spheres were the main products. At 500 °C for 10 h, many of the carbon nanotubes could be observed in the as-synthesized sample, as shown in Figure 2.

The experimental results suggest that the growth mechanism of the carbon nanotubes is clearly different from that of the early reports[20−23] that demonstrated that transition metal particles play a major role in the nucleation and growth of carbon nanotubes. Furthermore, a number of research groups reported that the catalytic particles were usually encapsulated at the tip of CNTs.[24−26] It is worth noting that there are no encapsulated solid particles in both kinds of carbon nanotubes, and the diameter (60−200 nm) of them is larger than that (1−4 nm) of CNTs in the previous literature,[27,28] suggesting a dissimilar formation mechanism. We observe that the carbon nanotubes always coexist with large sheets, as illustrated by the arrow in Figure 3C. This indicates the link between the nanotube and the sheet and corresponds with the spiral growth mechanism.[5] At the same time, we can find some curled belts, as shown in Figure 4A and B, which also confirms the spiral growth mechanism.

Conclusions

Carbon nanotubes and nanobelts have been synthesized by a medial-reduction route using metallic Mg powder as reductant. The reaction can be controlled easily because of the mild property of metallic Mg powder. It may provide a new method to produce carbon nanotubes under mild conditions. The carbon nanotubes obtained from our experiment have potential applications, such as gas or liquid channels and storage. However, much work is required to exactly understand the growth mechanism of carbon nanotubes.

Acknowledgment. This work is supported by the National Natural Science Foundation of China and 973 Projects of China. The authors gratefully acknowledge informative discussions with Professors Guien Zhou and Xianming Liu.

References and Notes

(1) Baughman, R. H.; Cui, C. X.; Zakhidov, A. A.; Iqbal, Z.; Barisci, J. N.; Spinks, G. M.; Wallace, G. G.; Mazzoldi, A.; De Rossi, D.; Rinzler, A. G.; Jaschinski, O.; Roth, S.; Kertesz, M. *Science* **1999**, *284*, 1340.

(2) Liu, C.; Fan, Y. Y.; Liu, M.; Cong, H. T.; Cheng, H. M.; Dresselhaus, M. S. *Science* **1999**, *286*, 1127.

(3) Shim, M.; Javey, A.; Kam, N. W. S.; Dai, H. J. *J. Am. Chem. Soc.* **2001**, *123*, 11512.

(4) Kim, P.; Lieber, C. M. *Science* **1999**, *286*, 2148.

(5) Iijima, S. *Nature* **1991**, *354*, 56.

(6) Fan, S.; Chapline, M. G.; Frank, N. R.; Tommbler, T. W.; Cassell, A. M.; Dai, H. *Science* **1999**, *283*, 512.

(7) Zhu, H. W.; Xu, C. L.; Wu, D. H.; Wei, B. Q.; Vajtai, R.; Ajayan, P. M. *Science* **2002**, *296*, 884.

(8) Maser, W. K.; Benito, A. M.; Martinez, M. T. *Carbon* **2002**, *40*, 1685.

(9) Peigney, A.; Coquay, P.; Flahaut, E.; Vandenberghe, R. E.; De Grave, E.; Laurent, C. *J. Phys. Chem. B* **2001**, *105*, 9699.

(10) Bethune, D. S.; Kiang, C. H.; deVries, M. S.; Gorman, G.; Savoy, R.; Vazquez, J.; Beyers, R. *Nature* **1993**, *363*, 605.

(11) Scott, C. D.; Arepalli, S.; Nikolaev, P.; Smalley, R. E. *Appl. Phys. A* **2001**, *72*, 573.

(12) Moreno, J. M. C.; Yoshimura, M. *J. Am. Chem. Soc.* **2001**, *123*, 741.

(13) O'Loughlin, J. L.; Kiang, C. H.; Wallace, C. H.; Reynolds, T. K.; Rao, L.; Kaner, R. B. *J. Phys. Chem. B* **2001**, *105*, 1921.

(14) Jiang, Y.; Wu, Y.; Zhang, S. Y.; Xu, C. Y.; Yu, W. C.; Xie, Y.; Qian, Y. T. *J. Am. Chem. Soc.* **2000**, *122*, 12383.

(15) Wang, X. J.; Lu, J.; Xie, Y.; Du, G.; Guo, Q. X.; Zhang, S. Y. *J. Phys. Chem. B* **2002**, *106*, 933.

(16) Zhang, H. B.; Lin, G. D.; Zhou, Z. H.; Dong, X.; Chen, T. *Carbon* **2002**, *40*, 2429.

(17) Klinke, C.; Kurt, R.; Bonard, J. M.; Kern, K. *J. Phys. Chem. B* **2002**, *106*, 11191.

(18) Dresselhaus, M. S.; Dresselhaus, G.; Pimenta, M. A.; Eklund, P. C. In *Analytical Applications of Raman Spectroscopy*; Pelletier, M. J., Ed.; Blackwell Science: Oxford, 1999; Chapter 9.

(19) Lee, Y. T.; Park, J.; Choi, Y. S.; Ryu, H.; Lee, H. J. *J. Phys. Chem. B* **2002**, *106*, 7614.

(20) Nerushev, O. A.; Morjan, R. E.; Ostrovskii, D. I.; Sveningsson, M.; Jonsson, M.; Rohmund, F.; Campbell, E. E. B. *Physica B* **2002**, *323*, 51.

(21) Dai, H. J.; Rinzler, A. G.; Nikolaev, P.; Thess, A.; Colbert, D. T.; Smalley, R. E. *Chem. Phys. Lett.* **1996**, *260*, 471.

(22) Diaz, G.; Benaissa, M.; Santiesteban, J. G.; Jose-Yacaman, M. *Fullerene Sci. Technol.* **1998**, *6*, 853.

(23) Terrones, M.; Grobert, N.; Zhang, J. P.; Terrones, H.; Olivares, J.; Hsu, W. K.; Hare, J. P.; Cheetham, A. K.; Kroto, H. W.; Walton, D. R. M. *Chem. Phys. Lett.* **1998**, *285*, 299.

(24) Jourdain, V.; Kanzow, H.; Castignolles, M.; Loiseau, A.; Bernier, P. *Chem. Phys. Lett.* **2002**, *364*, 27.

(25) Ducati, C.; Alexandrou, I.; Chhowalla, M.; Amaratunga, G. A. J.; Robertson, J. *J. Appl. Phys.* **2002**, *92*, 3299.

(26) Li, Y.; Chen, J.; Ma, Y.; Zhao, J.; Qin, Y.; Chang, L. *Chem. Commun.* **1999**, 1141.

(27) Yasuda, A.; Kawase, N.; Mizutani, W. *J. Phys. Chem. B* **2002**, *106*, 13294.

(28) Campbell, P. M.; Snow, E. S.; Novak, J. P. *Appl. Phys. Lett.* **2002**, *81*, 4586.